JTE
HCMUTE
ISSN: 2615-9740

JOURNAL OF TECHNICAL EDUCATION SCIENCE
Ho Chi Minh City University of Technology and Education
Website: https://jte.hcmute.edu.vn/index.php/jte/index
Email: jte@hcmute.edu.vn

# Nonlinear Controller with Dynamic Compensation for 6-DOF Manipulator in Practice

**Tran Minh Phuc, Ha Thanh Binh, Tong Hai Ninh, Tran Duc Thien***

*Department of Automatic Control, Ho Chi Minh City University of Technology and Education, Ho Chi Minh, Vietnam*
*Corresponding author. *Email: thientd@hcmute.edu.vn*

**ARTICLE INFO**

| | |
|---|---|
| Received: | 01/09/2022 |
| Revised: | 17/10/2022 |
| Accepted: | 04/11/2022 |
| Published: | 28/02/2023 |

**KEYWORDS**

Nonlinear controller;
Dynamic Compensation;
6-DOF manipulator;
PD control;
Lyapunov theory.

**ABSTRACT**

This paper presents a nonlinear controller with dynamic compensation for six degrees of freedom (6-DOF) manipulator Denso VS-6556 in practice. The manipulator is a complex nonlinear system with some limitations when applying a linear controller to control it. The nonlinear controller combines proportional derivative, and dynamic compensation is established to deal with this problem. The PD control is a linear controller, and dynamic compensation can cancel the nonlinear parts in the system. Therefore, the tracking problem is expected to result in a good performance. The stability and resilience of the entire system are examined using a Lyapunov technique. The test bench is built to ensure the conditions for experimentation; it includes card PCI QUAD04s, NI PCI-6713, industrial computer 610H Advantage, and MATLAB/Simulink in practice. Finally, the suggested control is subjected to the 6-DOF manipulator Denso 6556 and compared with the PD control to verify the effectiveness of the controller.

Doi: https://doi.org/10.54644/jte.75A.2023.1273



## 1. Introduction

A 6-DOF manipulator is a complex and strong nonlinear coupling system. In many different fields, it is commonly employed. In addition to taking the place of people working continuously and repeatedly, it also executes intelligent jobs much like a natural person. Robots have successfully achieved their missions in exploration, operating in hazardous environments, saving lives in accidents, and the diagnostic field of medicine because of their quick speeds and artificial intelligence. At the very least, the robots need appropriate controllers to satisfy the demands for precision and response speed to complete such a task. However, the critical challenges in developing high-precision controllers for robotic systems are dynamics complexity, model flaws, uncertain parameters, and noise from various real-world working environments. To overcome this problem, in simulation, some kinds of controllers were created to control precisely the robotic system, such as adaptive control [1]-[3], back-stepping control [1], [4]-[6], sliding mode control [2], [7]-[9], and neural control [10]-[13]. Although these controllers have been successfully used in several situations, they have significant drawbacks.

PID algorithms acting independently at each joint are used to drive most industrial robots. Although PID control has been proven effective in industrial practice for complex nonlinear systems like robots, some researchers contend [14] that PID control cannot handle highly nonlinear systems since the control law's construction is primarily based on local arguments created for the linearized system. Dealing with nonlinear systems is challenging because existing mathematical techniques do not provide us with strong enough tools to approach many issues we face analytically. Linearization is frequently utilized, reducing complexity and making something more manageable. The PD-plus-Gravity controller is an applicable controller in the computed torque control family based on linearization feedback compensation; this control law was treated in [15]. When the arm is at rest, Gravity is the only nonzero term in the dynamic, ignoring the disturbance in the system. [15] shown that the performance of the tracking task is improved when using PD-plus-Gravity than conventional PD.

In Vietnam, research on industrial robotic arms is also of great interest. In [16], authors build quasi-physical models and simulate them on MATLAB/Simscape. Applied the Computed Torque control for it on simulation, and the performance of the suggested modeling approach is proven through dynamics and control simulation on IRB 120. In [17], this paper presents focusing on solving the problem of inverse kinematics and the optimization algorithm in the parameter domain. Besides that, some controllers are applied to the manipulators, which have a lower degree of freedom to consider efficiency. In [18], the authors had been modeling and proposed a PD Folding set on a 4-degree-of-freedom robotic arm. Build 2 layers of artificial neural network for PD setting. Compare PD and PD Folding sets on simulation. However, the application of controllers to the 6-DOF manipulator is still limited.

This study applies a nonlinear controller with dynamic compensation to the 6-DOF manipulator to enhance the system's efficiency and precision. The test bench includes Denso VS-6556 combined with Data Acquisition (DAQ) systems NI PCI-6713, card QUAD04s, industrial computer 610H Advantech, and MATLAB/ Simulink. Moreover, the system's stability and sustainability with the proposed controller are also proven according to Lyapunov theory. Finally, some experiments on the controller were performed on a 6-DOF robotic arm, and the practice results were compared with conventional PD control to show that the suggested controller is more effective than the conventional PD control.

The rest of this study is as follows: In section 2, the test bench of the system in real life and the kinematics are shown, dynamic, and the design procedures of the nonlinear controller with dynamic compensation for the 6 DOF manipulator are presented in section 3, to demonstrate the stability of the entire system, a Lyapunov technique is applied. Some experiments will be performed in section 4. Finally, several conclusions and future works are discussed in section 5.

## 2. Materials and Methods

### *2.1. Experiment setup*

The experiment setup is shown in Figure 1, which includes an industrial computer 610H Advantech, PCI QUAD04s, a NI PCI-6713, a CPU Intel Core i5 6500, 1TB HDD, 12GB RAM, AC Servo motors, and MR J3-A drivers. The NI PCI-6713 is used to output the voltage from the algorithm on the computer to the drivers. The PCI QUAD04 measures the number of pulses from the encoder sensors to the MATLAB/Simulink modules of the industrial computer for handling MATLAB/Simulink supplied modules to interfaced PCIs.

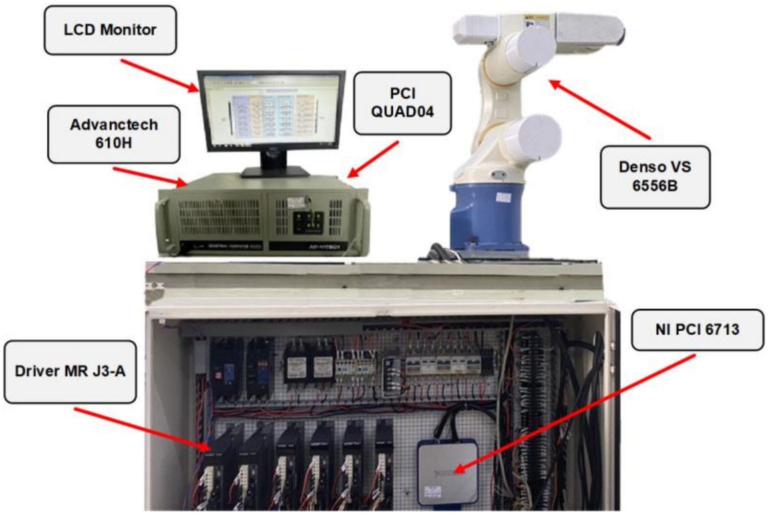


*a)*

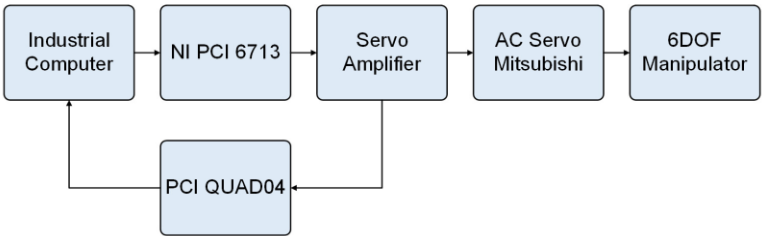


*b)*

**Figure 1.** *a) Description of the test bench in practice. b) The general diagram.*

### *2.2. Kinematics of 6-DOF manipulator*

Figure 1 and Figure 2, respectively, depict the link-frame assignments and the 6-DOF manipulator's construction. The mathematical description of the kinematic chain of the 6-DOF manipulators has been obtained using the Denavit-Hartenberg (DH) parameters notation, which indicates the degree of freedom and number of the link beginning in the basement.

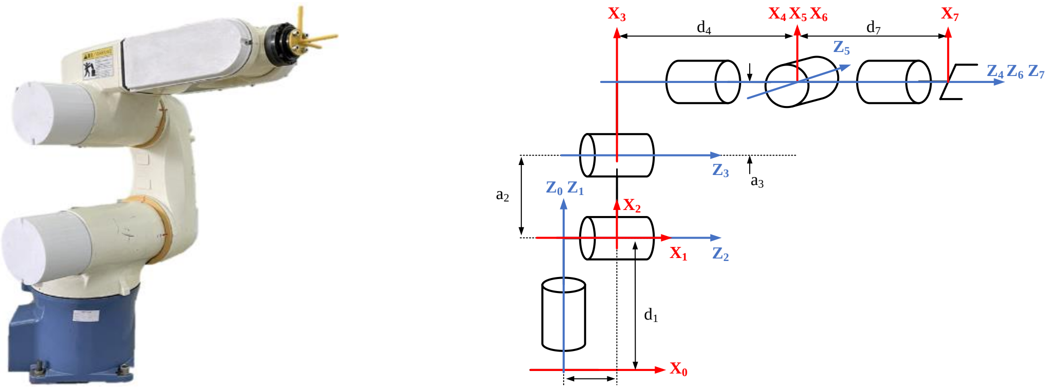


a) b)

**Figure 2**. *a) The experiment model in practice. b) The coordinate system of the 6-DOF manipulator.*

As depicted in Figure 2, the manipulator system has six joints and seven links, including the basement. The frame $\{i\}$ is attached rigidly to the link $i$, and the frame $\{E\}$ is referred to as the end-effector frame. The link parameters of DH conversion for the studied 6-DOF manipulator are shown in Table 1. Where $a_{i-1}$ is the link length, $\alpha_{i-1}$ denotes the link twist, $d_i$ is the link offset and $\theta_i$ is the angle of $i^{th}$ the joint.

**Table 1**. *The Denavit – Hartenberg table of the 6-DOF manipulator.*

| Link | $a_{i-1}$ | $\alpha_{i-1}$ | $d_i$ | $\theta_i$ | Range |
|---|---|---|---|---|---|
| 1 | 0 | 0 | $d_1$ | $\theta_1$ | ±170° |
| 2 | $a_1$ | –90° | 0 | $\theta_2 - 90°$ | –100° ÷135° |
| 3 | $a_2$ | 0 | 0 | $\theta_3$ | –119° +166° |
| 4 | $a_3$ | –90° | $d_4$ | $\theta_4$ | ±190° |
| 5 | 0 | 90° | 0 | $\theta_5$ | ±120° |
| 6 | 0 | –90° | 0 | $\theta_6$ | ±360° |
| E | 0 | 0 | 0 | $d_7$ | |

The following is the transformation matrix from the base frame to the end-effector frame:

$$ {}^{0}_{E}T = \begin{bmatrix} r_{11} & r_{12} & r_{13} & p_x \\ r_{21} & r_{22} & r_{23} & p_y \\ r_{31} & r_{32} & r_{33} & p_z \\ 0 & 0 & 0 & 1 \end{bmatrix} \quad (1) $$

The elements in (1) are presented in APPENDIX.S

JTE HCMUTE
ISSN: 2615-9740
**JOURNAL OF TECHNICAL EDUCATION SCIENCE**
Ho Chi Minh City University of Technology and Education
Website: https://jte.hcmute.edu.vn/index.php/jte/index
Email: jte@hcmute.edu.vn

### *2.3. Dynamics of the 6-DOF manipulator*

Consider a 6-DOF manipulator is depicted by joint space by:

$$\mathbf{M}(\boldsymbol{\theta})\ddot{\boldsymbol{\theta}} + \mathbf{C}(\boldsymbol{\theta},\dot{\boldsymbol{\theta}})\dot{\boldsymbol{\theta}} + \mathbf{g}(\boldsymbol{\theta}) = \boldsymbol{\tau} \tag{2}$$

Where $\boldsymbol{\theta},\dot{\boldsymbol{\theta}},\ddot{\boldsymbol{\theta}} \in \Re^{6\times1}$ display, in turn, the angular position, velocity, and acceleration vector in the manipulator's joint space; $\mathbf{M}(\boldsymbol{\theta}) \in \Re^{6\times6}$ presents the inertia matrix; $\mathbf{C}(\boldsymbol{\theta},\dot{\boldsymbol{\theta}}) \in \Re^{6\times6}$ expresses the Coriolis and centrifugal term matrix; $\mathbf{g}(\boldsymbol{\theta}) \in \Re^{6\times1}$ calculates the gravity vector, and $\boldsymbol{\tau} \in \Re^{6\times1}$ are torque terms.

**Property 1** [19]. $\dot{\mathbf{M}}(\boldsymbol{\theta})-2\mathbf{C}(\boldsymbol{\theta},\dot{\boldsymbol{\theta}})$ is a skew-symmetric matrix, so $\mathbf{z}^T\left[\dot{\mathbf{M}}(\boldsymbol{\theta})-2\mathbf{C}(\boldsymbol{\theta},\dot{\boldsymbol{\theta}})\right]\mathbf{z}=0$, where $\mathbf{z} \in \Re^{6\times1}$ is a vector.

**Assumption 1**: *The robot operates in the perfect environment with all dynamic and physical characteristics known.*

## 3. Control Design

Let define $\mathbf{x}_1 = \boldsymbol{\theta}$ and $\mathbf{x}_2 = \dot{\boldsymbol{\theta}}$; then tracking errors is defined as:

$$\mathbf{e} = \mathbf{x}_{1_d} - \mathbf{x}_1 \tag{3}$$

An applicable controller in the computed-torque family is the PD-plus-gravity controller that results when defined $\mathbf{g}(\mathbf{x}_1)$ as the gravity term of manipulator dynamics. To enhance the methods, after modifying the mathematic model of the 6-DOF manipulator, including the inertia matrix $\mathbf{M}(\mathbf{x}_1)$, the Coriolis and centrifugal term matrix $\mathbf{C}(\mathbf{x}_1,\mathbf{x}_2)$, and the gravity term, $\mathbf{g}(\mathbf{x}_1)$, then the proposed control to cancel the nonlinear term in the system is established.

Then, selecting PD feedback for $\mathbf{u}(t) \in \Re^{6\times1}$ yields

$$\mathbf{u} = \mathbf{K}_d\dot{\mathbf{e}} + \mathbf{K}_p\mathbf{e} + \mathbf{g}(\mathbf{x}_1) + \mathbf{M}(\mathbf{x}_1)\dot{\mathbf{x}}_{2_d} + \mathbf{C}(\mathbf{x}_1,\mathbf{x}_2)\mathbf{x}_{2_d} \tag{4}$$

, where $\mathbf{K}_p,\mathbf{K}_d \in \Re^{6\times6}$ are the positive diagonal matrix.

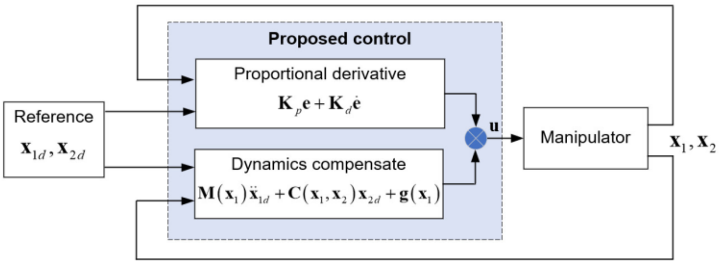


**Figure 3.** *The diagram of the proposed control.*

**Theorem 1**: *Suppose that the proposed control (4) is used. Then the tracking error (3) is zero.*

**Proof of the theorem 1:** Choose the Lyapunov function like below:

$$V = \frac{1}{2}\dot{\mathbf{e}}^T\mathbf{M}(\mathbf{x}_1)\dot{\mathbf{e}} + \frac{1}{2}\mathbf{e}^T\mathbf{K}_p\mathbf{e} \tag{5}$$

Taking the derivative of the Lyapunov function

$$\begin{aligned}\dot{V} &= \dot{\mathbf{e}}^T\left(-\mathbf{C}(\mathbf{x}_1,\mathbf{x}_2)\dot{\mathbf{e}} - \mathbf{K}_p\mathbf{e} - \mathbf{K}_d\dot{\mathbf{e}}\right) + \frac{1}{2}\dot{\mathbf{e}}^T\dot{\mathbf{M}}\dot{\mathbf{e}} + \dot{\mathbf{e}}^T\mathbf{K}_p\mathbf{e} \\ &= \dot{\mathbf{e}}^T\left(-\mathbf{K}_d\dot{\mathbf{e}} - \mathbf{K}_p\mathbf{e} - \mathbf{C}(\mathbf{x}_1,\mathbf{x}_2)\dot{\mathbf{e}}\right) + \frac{1}{2}\dot{\mathbf{e}}^T\dot{\mathbf{M}}(\mathbf{x}_1)\dot{\mathbf{e}} + \dot{\mathbf{e}}^T\mathbf{K}_p\mathbf{e} \\ &= \frac{1}{2}\left(\dot{\mathbf{e}}^T\left(\dot{\mathbf{M}}(\mathbf{x}_1) - 2\mathbf{C}(\mathbf{x}_1,\mathbf{x}_2)\right)\dot{\mathbf{e}}\right) - \dot{\mathbf{e}}^T\mathbf{K}_d\dot{\mathbf{e}}\end{aligned} \tag{6}$$

By applying **Property 1**, then the derivative of the Lyapunov function is calculated as:

$$\dot{V} = -\dot{\mathbf{e}}^{\mathrm{T}}\mathbf{K}_d\dot{\mathbf{e}} < 0 \tag{7}$$

Based on the Lyapunov theorem, the system is stable. Then **Theorem 1** is proved.

## 4. Results and Discussion

### *4.1. Experiment Description*

To ensure the accuracy and appropriateness of the suggested control to the 6-DOF manipulator model, as shown in Figure 1. The parameters in detail are shown in Table 2.

**Table 2**. *The parameters of the system.*

| Variables | Description | Variables | Description |
|---|---|---|---|
| $a_1 = 0.0075(m)$ | Distance between $z_0$-axis and $z_2$- axis | $m_1 = 5.65(Kg)$ | Weight of link 1 |
| $a_2 = 0.27(m)$ | Distance between $z_2$-axis and $z_3$- axis | $m_2 = 4.6(Kg)$ | Weight of link 2 |
| $a_3 = 0.09(m)$ | Distance between $z_3$-axis and $z_5$- axis | $m_3 = 4.3(Kg)$ | Weight of link 3 |
| $d_1 = 0.335(m)$ | Distance between $x_0$-axis and $x_1$- axis | $m_4 = 1.9151(Kg)$ | Weight of link 4 |
| $d_4 = 0.295(m)$ | Distance between $x_3$-axis and $x_4x_5x_6$- axis | $m_5 = 0.4(Kg)$ | Weight of link 5 |
| $d_7 = 0.08(m)$ | Distance between $x_4$-axis and $x_7$- axis | $m_6 = 0.0714(Kg)$ | Weight of link 6 |

The robot manipulator's initial position was set to $\mathbf{x}_1(0) = [0 \quad 0 \quad 0 \quad 0 \quad 0 \quad 0]^T(\deg)$, and $\mathbf{x}_2(0) = [0 \quad 0 \quad 0 \quad 0 \quad 0 \quad 0]^T(\deg.s^{-1})$. The desired trajectory for each joint is set the same as:

$$\mathbf{x}_{1_d} = 30\sin(2\pi ft)(\deg) \tag{8}$$

Where the amplitude of each joint is equal to 30 degrees with *f* as the frequency and *t* as the operating time, the sampling time of 0.01 seconds, the simulation time of 30 seconds, and $f = 0.1(\text{Hz})$.

**Remark 1:** The recommended control is contrasted with the standard PD control to verify the productivity of the proposed control.

The PD control law:

$$\mathbf{u}_{PD} = \mathbf{K}_p\mathbf{e} + \mathbf{K}_d\dot{\mathbf{e}} \tag{9}$$

The Proposed control law:

$$\mathbf{u} = \mathbf{K}_p\mathbf{e} + \mathbf{K}_d\dot{\mathbf{e}} + \mathbf{M}(\mathbf{x}_1)\ddot{\mathbf{x}}_{1_d} + \mathbf{C}(\mathbf{x}_1,\mathbf{x}_2)\dot{\mathbf{x}}_{1_d} + \mathbf{g}(\mathbf{x}_1) \tag{10}$$

**Remark 2**: The trial-error method chooses the PD control and proposed control coefficients. They have the same value since they have the same components as the linear controller, and the difference between them is the dynamic compensation term of the proposed control to cancel the nonlinear part of the system. The coefficient is shown in Table 3.

**Table 3**. *The coefficient of controllers.*

| Controllers | Control Parameters |
|---|---|
| **PD** | $\mathbf{K}_p = diag([45 \quad 60 \quad 65 \quad 80 \quad 100 \quad 120])$<br>$\mathbf{K}_d = diag([0.7 \quad 0.8 \quad 0.65 \quad 0.5 \quad 0.8 \quad 1.2])$ |
| **Proposed Control** | $\mathbf{K}_p = diag([45 \quad 60 \quad 65 \quad 80 \quad 100 \quad 120])$<br>$\mathbf{K}_d = diag([0.7 \quad 0.8 \quad 0.65 \quad 0.5 \quad 0.8 \quad 1.2])$ |

JTE
HCMUTE
ISSN: 2615-9740
JOURNAL OF TECHNICAL EDUCATION SCIENCE
Ho Chi Minh City University of Technology and Education
Website: https://jte.hcmute.edu.vn/index.php/jte/index
Email: jte@hcmute.edu.vn

### *4.2. Experimental results*

Figure 4 shows the response at each joint to the input signal. The black line presents the reference. The blue dot-line is a response when the proportional derivative control is used, and the red dot-line is a proposed control. All the output signals track with the reference input signals.

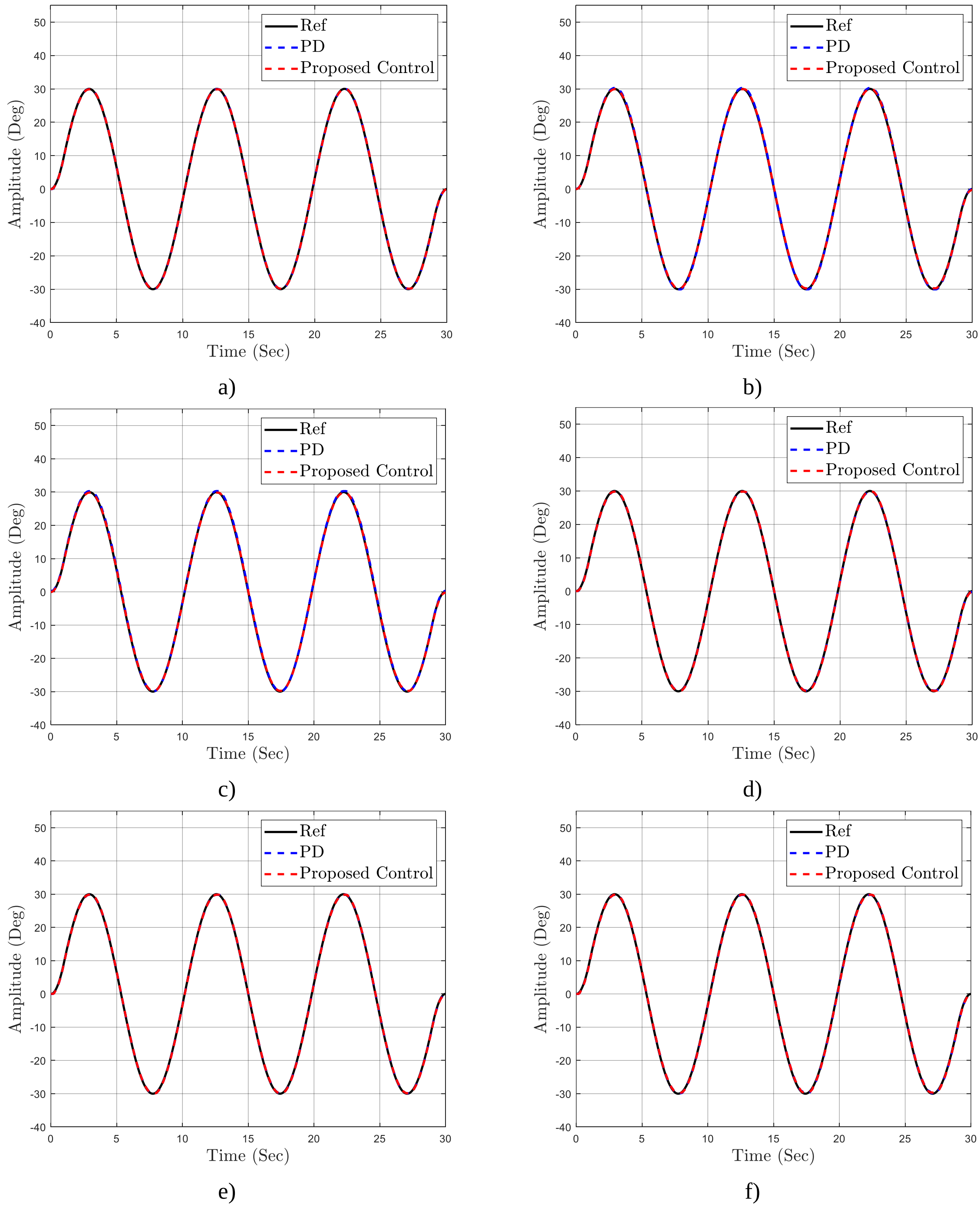


**Figure 4.** *The output response of the manipulator with PD and Proposed control in a) joint 1, b) joint 2, c) joint 3, d) joint 4, e) joint 5, and f) joint 6.*

To declare the performance of each controller, Figure 5 presents the error efforts at each joint, in turn, by blue lines of PD and red lines of the proposed control. Looking at the tracking errors at joints $2^{th}$ and $3^{th}$, with the proposed control, the system's performance is enhanced than with the PD control. When the robot arm is at rest or working, the nonlinear terms that affect the system are destroyed because of the dynamic compensation in the control law.

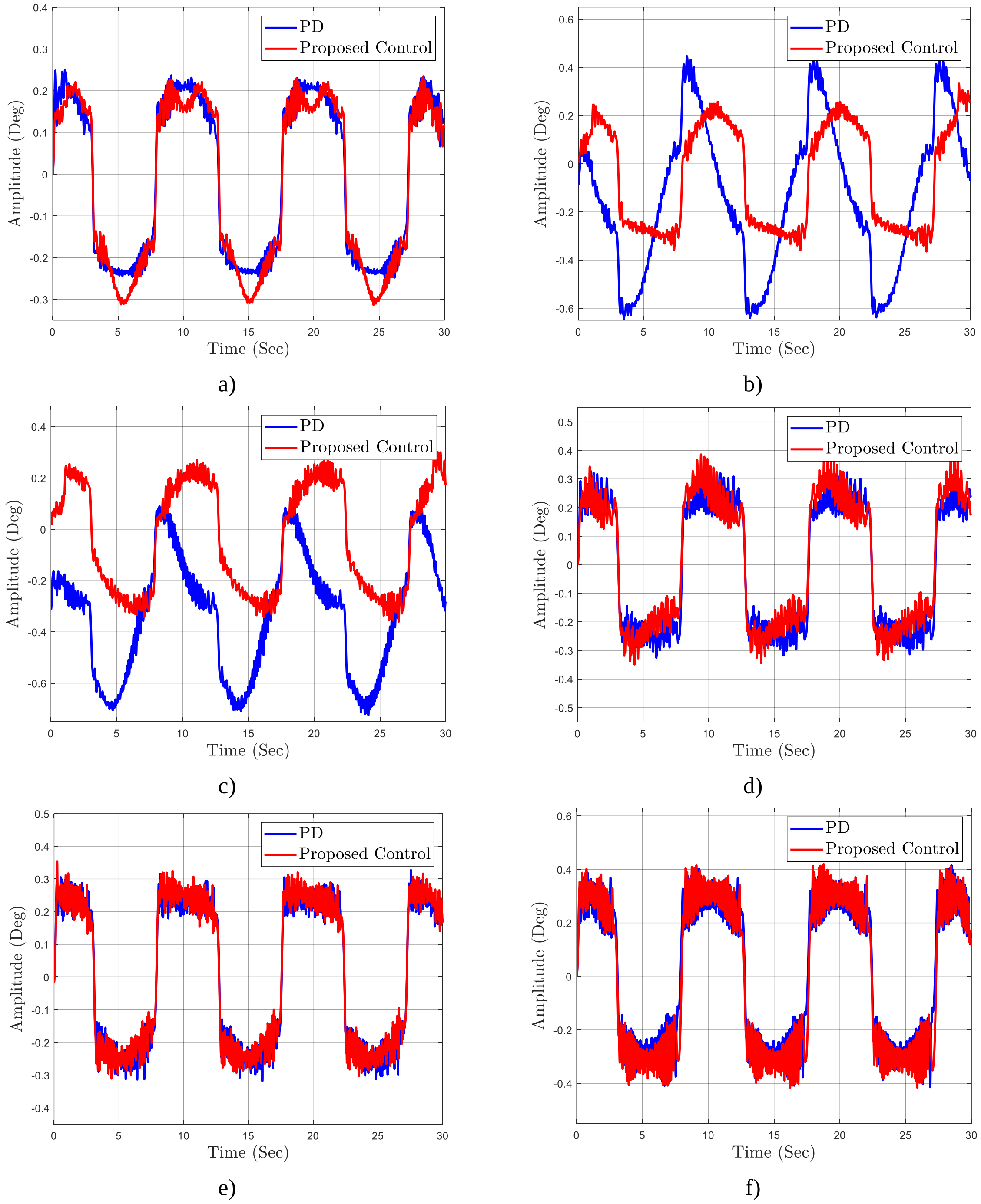


**Figure 5**. *Control signals responses of the manipulator with PD and Proposed control in a) joint 1, b) joint 2, c) joint 3, d) joint 4, e) joint 5, and f) joint 6.*

## 5. Conclusions

This paper presented a nonlinear controller with dynamic compensation applied to the 6-DOF manipulator to enrich the performance and precision of the system in practice. The test bench is built, including the Denso VS-6556 model combined with Data Acquisition (DAQ) systems NI PCI-6713, PCI QUAD04s, industrial computer 610H Advantech, and interfaced via MATLAB/ Simulink. The stability and robustness of the system with the proposed control were verified in theory using the Lyapunov approach. Finally, the proposed control was applied to the 6-DOF manipulator test bench. The results of the proposed controller were compared with the PD controller to demonstrate its effectiveness.

However, the parameters in most physical systems, such as robot manipulators, are unknown or time-variant. Therefore, in the future, several adaptive or robustness controllers will be created and applied to this manipulator in practice to deal with this problem.

## APPENDIX

$$\begin{aligned}
r_{11} &= s_6\left(s_1c_4 - c_1s_{23}s_4\right) + c_6\left(\left(s_1s_4 + c_1s_{23}c_4\right)c_5 + c_1c_{23}s_5\right)\\
r_{12} &= c_6\left(s_1c_4 - c_1s_{23}s_4\right) - s_6\left(\left(s_1s_4 + c_1s_{23}c_4\right)c_5 + c_1c_{23}s_5\right)\\
r_{13} &= c_1c_{23}c_5 - \left(s_1s_4 + c_1s_{23}c_4\right)s_5\\
r_{21} &= -s_6\left(c_1c_4 + s_1s_{23}s_4\right) - c_6\left(\left(c_1s_4 + s_1s_{23}c_4\right)c_5 - s_1c_{23}s_5\right)\\
r_{22} &= s_6\left(\left(c_1s_4 - s_1s_{23}c_4\right)c_5 - s_1c_{23}s_5\right) - c_6\left(c_1c_4 + s_1s_{23}s_4\right)\\
r_{23} &= \left(c_1s_4 - s_1s_{23}c_4\right)s_5 + s_1c_{23}c_5\\
r_{31} &= -\left(s_{23}s_5 - c_{23}c_4c_5\right)c_6 - c_{23}s_4s_6\\
r_{32} &= \left(s_{23}s_5 - c_{23}c_4c_5\right)s_6 - c_{23}s_4c_6\\
r_{33} &= -s_{23}c_5 - c_{23}c_4s_5\\
p_x &= c_1\left(a_1 + d_4c_{23} + a_3s_{23} + a_2s_2\right) - d_7\left(\left(s_1s_4 + c_1s_{23}c_4\right)s_5 - c_1c_{23}c_5\right)\\
p_y &= s_1\left(a_1 + d_4c_{23} + a_3s_{23} + a_2s_2\right) + d_7\left(\left(c_1s_4 - s_1s_{23}c_4\right)s_5 + s_1c_{23}c_5\right)\\
p_z &= d_1 + a_3c_{23} - d_4s_{23} - d_7\left(s_{23}c_5 + c_{23}c_4s_5\right) + a_2c_2
\end{aligned} \quad (11)$$

Where $s(.) \triangleq \sin(.),\ c(.) \triangleq \cos(.), s_{23} \triangleq \sin(\theta_2+\theta_3), c_{23} \triangleq \cos(\theta_2+\theta_3)$.

## Acknowledgments

This research was implemented at Robotics and Intelligent Control Laboratory (RIC Lab), Faculty of Electrical and Electronics Engineering, Ho Chi Minh City University of Technology and Education, Vietnam.

## REFERENCES

[1] N. Nikdel, M. A. Badamchizadeh, V. Azimirad, and M. A. Nazari, "Adaptive back-stepping control for an n-degree of freedom robotic manipulator based on combined state augmentation," *Robotics and Computer-Integrated Manufacturing*, vol. 44, pp. 129-143, 2017, doi: 10.1016/j.rcim.2016.08.007.

[2] T. D. Thien, D. M. Tri, and T. T. Luong, "Adaptive sliding mode control design with genetic algorithm for a 2-DOF robotic manipulator with uncertainties," in *the 6th International Conference and Exhibition on Control and Automation*, Vietnam, 2022, Paper 37.

[3] T. Yang, N. Sun, Y. Fang, X. Xin, and H. Chen, "New Adaptive Control Methods for $n$-Link Robot Manipulators With Online Gravity Compensation: Design and Experiments," *IEEE Transactions on Industrial Electronics*, vol. 69, no. 1, pp. 539-548, 2022, doi: 10.1109/tie.2021.3050371.

[4] H. J. Kang *et al.*, "A Backstepping Global Fast Terminal Sliding Mode Control for Trajectory Tracking Control of Industrial Robotic Manipulators," *IEEE Access*, vol. 9, pp. 31921-31931, 2021, doi: 10.1109/ACCESS.2021.3060115.

[5] T. D. Thien *et al*., "A Finite -Time Robust Control for a Manipulator with Output Constraints and Unknown Control Directions," in *2020 5th International Conference on Green Technology and Sustainable Development (GTSD)*, Nov. 2020, pp. 185-191, doi: 10.1109/GTSD50082.2020.9303058.

[6] T. D. Thien, M. Jin, and K. K. Ahn, "Nonlinear Extended State Observer Based on Output Feedback Control for a Manipulator With Time-Varying Output Constraints and External Disturbance," *IEEE Access*, vol. 7, pp. 156860-156870, 2019, doi: 10.1109/ACCESS.2019.2949594.

[7] K. Lochan, S. Suklabaidya, and B. K. Roy, "Sliding mode and adaptive sliding mode control approaches of two link flexible manipulator," in *Proceedings of the 2015 Conference on Advances In Robotics - AIR '15*, 2015, pp. 1-6.

[8] T. D. Thien and N. T. Quang, "Fault-Tolerant Sliding Mode Controller For a 4 Degree of Freedom Robotic Manipulator," in *13th Asian Control Conference (ASCC)*, May 2022, pp. 1347-1352, doi: 10.23919/ASCC56756.2022.9828134.

[9] T. D. Thien, D. T. Cuong, and K. K. Ahn, "Extended High Gain Observer-Based Sliding Mode Control for an Electro-hydraulic System with a Variant Payload," *International Journal of Precision Engineering and Manufacturing*, vol. 20, no. 12, pp. 2089-2100, 2019, doi: 10.1007/s12541-019-00256-0.

[10] Q. Guo, Y. Zhang, B. G. Celler, and S. W. Su, "Neural Adaptive Backstepping Control of a Robotic Manipulator With Prescribed Performance Constraint," *IEEE Trans. Neural Netw. Learn Syst.*, vol. 30, no. 12, pp. 3572-3583, Dec. 2019, doi: 10.1109/TNNLS.2018.2854699.

[11] V. A. Tuan and H. J. Kang, "Adaptive Neural Integral Full-Order Terminal Sliding Mode Control for an Uncertain Nonlinear System," *IEEE Access*, vol. 7, pp. 42238-42246, 2019, doi: 10.1109/ACCESS.2019.2907565.

[12] V. A. Tuan and H. J. Kang, "An Adaptive Terminal Sliding Mode Control for Robot Manipulators With Non-Singular Terminal Sliding Surface Variables," *IEEE Access*, vol. 7, pp. 8701-8712, 2019.

[13] T. H. Vu *et al*., "Adaptive Fuzzy Backstepping Sliding Mode Control for a 3-DOF Hydraulic Manipulator with Nonlinear Disturbance Observer for Large Payload Variation," *Applied Sciences,* vol. 9, no. 16, 2019, doi: 10.3390/app9163290.
[14] J. T. Wen and D. S. Bayard, "New class of control laws for robotic manipulators Part 1. Non–adaptive case," *International Journal of Control,* vol. 47, no. 5, pp. 1361-1385, 1988, doi: 10.1080/00207178808906102.
[15] M. Takegaki and S. Arimoto, "A New Feedback Method for Dynamic Control of Manipulators," *Journal of Dynamic Systems, Measurement, and Control,* vol. 103, no. 2, pp. 119-125, 1981, doi: 10.1115/1.3139651.
[16] L. N. Truc and N. T. Lam, "Quasi-physical modeling of robot IRB 120 using Simscape Multibody for dynamic and control simulation," *Turkish Journal of Electrical Engineering & Computer Sciences,* vol. 28, no. 4, pp. 1949-1964, 2020, doi: 10.3906/elk-1909-131.
[17] X. B. Duong, A. T. Phan, D. N. Do, X. H. Dang, K. N. Truong, and N. A. Mai, "Optimize the Feed Rate and Determine the Joints Torque for Industrial Welding Robot TA 1400 Based on Kinematics and Dynamics Modeling," *International Journal of Mechanical Engineering and Robotics Research,* pp. 1335-1340, 2020, doi: 10.18178/ijmerr.9.9.1335-1340.
[18] V. T. Tai, D. N. Minh, and D. X. Ba, "A PD-Folding-Based Controller for a 4DOF Robot," in *International Conference on Green Technology and Sustainable Development*, 2020, pp. 117-129.
[19] L. N. Truc, N. V. Quyen, and N. P. Quang, "Dynamic Model with a New Formulation of Coriolis/Centrifugal Matrix for Robot Manipulators," *Journal of Computer Science and Cybernetics,* vol. 36, no. 1, pp. 89-104, 2020, doi: 10.15625/1813-9663/36/1/14557.

**MINH PHUC TRAN** received the B.S degree in the Department of Automation Control, Ho Chi Minh University of Technology and Education, Vietnam, in 2022.

He works as a member of Robotics and Intelligent Control Lab in the Department of Automatic Control, Ho Chi Minh City University of Technology and Education (HCMUTE), Vietnam.

His research interests include robotics, nonlinear control, adaptive control, and fault-tolerant control.

**THANH BINH HA** received the B.S degree in the Department of Automation Control, Ho Chi Minh University of Technology and Education, Vietnam, in 2022.

He works as a member of Robotics and Intelligent Control Lab in the Department of Automatic Control, Ho Chi Minh City University of Technology and Education (HCMUTE), Vietnam.

His research interests include robotics, nonlinear control, adaptive control, and fault-tolerant control.

**HAI NINH TONG** received the B.S degree in the Department of Automation Control, Ho Chi Minh University of Technology and Education, Vietnam, in 2022.

He works as a member of Robotics and Intelligent Control Lab in the Department of Automatic Control, Ho Chi Minh City University of Technology and Education (HCMUTE), Vietnam.

His research interests include robotics, nonlinear control, adaptive control, and fault-tolerant control.

**DUC THIEN TRAN** received the B.S and M.S. degrees in the Department of Electrical Engineering, Ho Chi Minh City University of Technology, Vietnam, in 2010, 2013, and the Ph.D. degree from University of Ulsan in 2020, respectively.

He works as a lecturer with the Department of Automatic Control, Ho Chi Minh City University of Technology and Education (HCMUTE), Vietnam.

His research interests include robotics, variable stiffness system, fluid power control, disturbance observer, nonlinear control, adaptive control, fault tolerant control and intelligent technique.